Conventional Kinesin Holoenzymes Are Composed of Heavy and Light Chain Homodimers[†]

Scott R. DeBoer,[‡,§] YiMei You,[‡,§] Anita Szodorai,[||] Agnieszka Kaminska,[§] Gustavo Pigino,[§] Evelyn Nwabuisi,[§] Bin Wang,[§] Tatiana Estrada-Hernandez,[§] Stefan Kins,[||] Scott T. Brady,[§] and Gerardo Morfini*[,§]

Department of Anatomy and Cell Biology, University of Illinois at Chicago, Chicago, Illinois 60612, and Center for Molecular Biology, University of Heidelberg (ZMBH), Heidelberg, Germany

Received December 14, 2007; Revised Manuscript Received February 24, 2008

ABSTRACT: Conventional kinesin is a major microtubule-based motor protein responsible for anterograde transport of various membrane-bounded organelles (MBO) along axons. Structurally, this molecular motor protein is a tetrameric complex composed of two heavy (kinesin-1) chains and two light chain (KLC) subunits. The products of three kinesin-1 (kinesin-1A, -1B, and -1C, formerly KIF5A, -B, and -C) and two KLC (KLC1, KLC2) genes are expressed in mammalian nervous tissue, but the functional significance of this subunit heterogeneity remains unknown. In this work, we examine all possible combinations among conventional kinesin subunits in brain tissue. In sharp contrast with previous reports, immunoprecipitation experiments here demonstrate that conventional kinesin holoenzymes are formed of kinesin-1 homodimers. Similar experiments confirmed previous findings of KLC homodimerization. Additionally, no specificity was found in the interaction between kinesin-1s and KLCs, suggesting the existence of six variant forms of conventional kinesin, as defined by their gene product composition. Subcellular fractionation studies indicate that such variants associate with biochemically different MBOs and further suggest a role of kinesin-1s in the targeting of conventional kinesin holoenzymes to specific MBO cargoes. Taken together, our data address the combination of subunits that characterize endogenous conventional kinesin. Findings on the composition and subunit organization of conventional kinesin as described here provide a molecular basis for the regulation of axonal transport and delivery of selected MBOs to discrete subcellular locations.

Molecular motors of the kinesin and dynein superfamilies are responsible for microtubule- (MT-) based motility in cells. Approximately 40–45 kinesin-related polypeptides have been identified in mouse and human (*1*), with 25 or more being expressed in the developing nervous system (*2*). From these, conventional kinesin is the most abundant kinesin family member in the adult nervous system (*3*). Biochemical (*4*) and electron microscopic studies (*5*) indicated that the native conventional kinesin holoenzyme exists as a tetramer consisting of two kinesin light chain (KLCs)[1] and two kinesin heavy chain (kinesin-1, KHC, KIF5s) subunits (*6*). Following the agreed nomenclature for kinesins, the term "conventional kinesin" herein refers to the tetrameric motor protein complex (heavy and light chains), whereas "kinesin-1" refers exclusively to the heavy chain subunits (*7*). Experimental evidence indicates that KLCs play a role in the binding (*8*) and targeting (*9*) of conventional kinesin to MBOs through interactions involving their tandem repeat (TR) domain (*10*) and their alternatively spliced carboxy terminus (*8, 11, 12*), respectively. Kinesin-1s, on the other hand, are responsible for the mechanochemical properties of the conventional kinesin holoenzyme, containing both MT binding and ATPase domains at their amino terminus (*4*). Following the amino-terminal motor domain, a hinge, a stalk, and a globular tail are found toward the carboxy terminus of kinesin-1s (*13*). While the stalk region mediates their interaction with KLCs (*14*), the variable globular tail of kinesin-1 has been proposed to play a role in the regulation and cargo targeting of conventional kinesin (*9, 13*) and to provide an interaction site for other proteins, such as myosin V (*15*). Although ultrastructural studies suggest an association of both the kinesin-1 tail domain and KLCs with their transported cargoes (*16*), little is known about the precise roles that each subunit plays in this process (*13*).

In neuronal cells, conventional kinesin is a major MT-based motor responsible for the anterograde transport of various membrane-bound organelles (MBOs) from the neuronal cell body to their final sites of utilization in axons (*17, 18*). MBOs associated with conventional kinesin include mitochondria, synaptic vesicle precursors, lysosomes, and post-Golgi vesicle carriers (*19–21*). Intriguingly, these MBOs differ significantly in their biochemical composition and transport rates (*18*). Moreover, different MBO cargoes

[†] This work was supported by grants from the Huntington's Disease Society of America (HDSA) and ALSA (to G.M.), grants from NINDS (NS23868, NS23320, NS41170 and NS43408), MDA, and ALSA (to S.T.B.), and the Fitz-Thyssen Foundation and DFG (to S.K.).

* To whom correspondence should be addressed. Phone: (312) 996-6791. Fax: (312) 413-0354. E-mail: gmorfini@uic.edu.

[‡] These authors contributed equally to this paper.

[§] University of Illinois at Chicago.

[||] University of Heidelberg.

[1] Abbreviations: KHC, kinesin heavy chain; KLC, kinesin light chain; TR, tandem repeats; PIPES, 1,4-piperazinediethanesulfonic acid; HEPES, *N*-(2-hydroxyethyl)piperazine-*N*′-2-ethanesulfonic acid; AMP-PNP, adenosine 5′-(β,γ-imino)triphosphate; GST, glutathione *S*-transferase; SDS−PAGE, sodium dodecyl sulfate−polyacrylamide gel electrophoresis; ECL, enchanced chemiluminescence; PVDF, poly(vinylidene difluoride); MBO, membrane-bound organelle.

10.1021/bi702445j CCC: $40.75
Published on Web 03/25/2008

often need to be delivered to distinct, specialized axonal subdomains. Neurotransmitter-bearing synaptic vesicles and their precursors, for example, are delivered in a regulated fashion to presynaptic terminals, whereas vesicles bearing specific sodium channels need to be selectively delivered to nodes of Ranvier (*22*). These observations suggest the existence of molecular mechanisms that allow for the targeting of conventional kinesin to biochemically heterogeneous MBO cargoes and for the regulation of their delivery to specific axonal domains (*23*).

Recently, genetic information revealed a significant heterogeneity among the composing subunits of conventional kinesin (*2*). Specifically, three kinesin-1 genes [kinesin-1A, kinesin-1B, and kinesin-1C, formerly known as KIF5A, -B, and -C (*7*)] and two KLC genes [KLC1 and KLC2 (*24*)] have been identified in mammalian nervous tissue. Although the biological significance of this heterogeneity in conventional kinesin subunits is unknown, it might play a role in the selective targeting of conventional kinesin to different cargoes (*13*) and in the differential regulation of their transport by effector proteins (*25*). Earlier studies provided partial information on the interaction among selected subunits of conventional kinesin (*24, 26, 27*). However, the combination of subunits that generates biochemically heterogeneous forms of conventional kinesin has not yet been addressed.

To gain novel insights on the biochemical heterogeneity of conventional kinesin, we performed immunoprecipitation experiments using well-validated, highly specific antibodies that selectively recognize each kinesin-1 and KLC subunit. Data presented here demonstrates that endogenous conventional kinesin from brain is exclusively composed of kinesin-1 and KLC homodimers. No selectivity was found in the interaction between kinesin-1 and KLC homodimers, suggesting the existence of six subunit combinations that give rise to biochemically heterogeneous forms of conventional kinesin. Subcellular fractionation studies also indicated that different subunit variants of conventional kinesin associate with different MBOs and suggested a potential role of kinesin-1s in their MBO targeting. Our findings on subunit-dependent heterogeneity of conventional kinesin and their homodimerization properties provide a molecular basis for the transport regulation of selected MBOs in neurons.

EXPERIMENTAL PROCEDURES

Recombinant Proteins. Full-length cDNAs coding for mouse kinesin-1A, -1B, and -1C were subcloned into pcDNA-myc-6His plasmid vector (Invitrogen, San Diego, CA). COS-7 cells were transiently transfected using Lipofectamine reagent (*28*) for 24 h, as indicated by the manufacturer. A GST-tagged polypeptide comprising amino acids 1–535 of murine kinesin-1B (GST-KIF5B1–535; a generous gift from P. Ferreira) was expressed and purified as described before (*25*).

Antibody Production. Peptide sequences unique for each kinesin-1 (see Table 1) were identified and synthesized (Biosynthesis) with an additional cysteine residue located at the amino terminus. These peptides were conjugated to keyhole lympet hemocyanin and injected into rabbits or mice (Pierce). Rabbit polyclonal anti-KIF5B sera were generated in rabbits (Cocalico) and affinity purified from whole serum using recombinant GST-KIF5B1–535 conjugated to cyanogen bromide-activated Sepharose beads (*25*). Monoclonal antibodies against kinesin-1C (uKHC) and KLC2 (B2A5) were produced as described before (*10, 29*).

Antibodies. A detailed description of anti-kinesin-1 and anti-KLC antibodies used here is provided in Table 1. Unless indicated, antibody stocks were prepared at 1 mg/mL concentration and used at the following concentrations: anti-KIF5A, 1:1000 (Affinity BioReagents catalog no. PA1–642); anti-KIF5B, 1:1000 (Affinity BioReagents catalog no. PA1–643); anti-KIF5B (UIC 81), 1:500; anti-KIF5C (uKHC), 1:1000; anti-(pan) kinesin-1 (H2, Chemicon), 1:1000; anti-pan KLC (63–90), 1:500; anti-pan KLC (KLC-All), 1:500; anti-KLC1 (L2, 1:500; anti-KLC2 (B2A5), 1:500; anti-SNAP-25, 1:2500 (Santa Cruz sc-20048); anti-6-His tag (Qiagen), 1:500; rabbit anti-synapsin-1, 1:5000 (BioTrend); mouse anti-synaptophysin, 1:500 (Sigma); mouse anti-APP, 1:5000 (22C11, Roche); and rabbit anti-synaptotagmin (Sigma), 1:5000. The following secondary antibodies were used: Jackson 111-035-045 HRP-conjugated goat anti-rabbit, 1:15000, and Jackson 115-035-146 HRP-conjugated goat anti-mouse IgG, 1:15000.

Immunoblots. Proteins were separated by SDS−PAGE on 4–12% Bis-Tris gels (NuPage minigels; Invitrogen) using MOPS running buffer (Invitrogen) and transferred to PVDF using Towbin buffer supplemented with 10% (v/v) methanol (90 min at 400 mA using a Hoeffer TE22 apparatus). Immunoblots were blocked with 1% (w/v) non-fat dried milk in PBS (12 mM sodium phosphate, pH 7.4, 1.4 mM potassium phosphate, 2.7 mM potassium chloride, and 140 mM NaCl). Membranes were incubated with primary antibodies overnight at 4 °C in 1% IgG-free BSA and washed four times with 0.1% Tween-20 in PBS. Primary antibody binding was detected with HRP-conjugated anti-mouse or anti-rabbit antibody (Jackson Immunoresearch) and visualized by chemiluminescence (ECL; Amersham). The molecular mass marker was from Invitrogen (Blue Plus2 prestained standard no. LC5925).

Microtubule Pellet Preparation. Conventional kinesin-enriched microtubule (MT) pellets were prepared as described before (*30*). Mouse brains were dissected and quickly homogenized in BRB80 buffer (80 mM PIPES, pH 6.8, 1 mM $MgCl_2$, and 1 mM EDTA, pH 7) containing mammalian protease inhibitor cocktail (1:100 dilution; Sigma). This homogenate was centrifuged at $12500g_{max}$ for 20 min at 4 °C. The supernatant fraction was transferred to a new tube and centrifuged at $125000g_{max}$ for 5 min at 4 °C in a TL100.3 rotor (Beckman). The resulting supernatant (cytosol) was transferred to a new tube and adjusted to 20 μM Taxol and either 2 mM ATP or 2 mM AMP-PNP. After 30 min at 37 °C, MT-containing cytosolic fractions were loaded on top of a 20% sucrose cushion prepared in BRB80 buffer plus 20 μM Taxol and centrifuged at 35000 rpm ($131438g_{max}$) in a MLS-50 rotor (Beckman) for 10 min. The resulting MT pellets were resuspended in BRB80 using a 27 gauge syringe. Pellets and supernatant fractions were adjusted to 1× gel loading buffer (GLB) using a 5× GLB stock [0.35 M Tris-HCl, pH 6.8, 10% (w/v) SDS (Pierce, Sequanal grade), 36% glycerol, 5% β-mercaptoethanol, 0.01% bromophenol blue], as previously described (*31*).

Immunoprecipitation Experiments. Mouse brains were homogenized in lysis buffer [LB; 25 mM Tris-HCl, pH 7.4, 150 mM NaCl, 1% Triton X-100, and 1/100 dilution of

Table 1: Characteristics of Anti-Kinesin-1 and Anti-KLC Antibodies Used in This Study[a]

Antibody	Specificity	Source	Host	Immunogen/Epitope	Sp. Specif.	*Ref.*
PA1-642	Kinesin-1A	Affinity Bioreagents *Abcam (ab5628)	Rabbit, polyclonal	**1008-**GYEAEDQAKLFPLHQETAAS**-1027**	M,R,H	*This work*
PA1-643	Non-Specific ~100 kD protein	Affinity Bioreagents *Abcam (ab5629)	Rabbit, polyclonal	**376-**IDEQFDKEKANLEAFTVDKDI**-396**	ND	*This work*
UIC 81	Kinesin-1B	NA	Rabbit, polyclonal	**387-**LEAFTADKDIAITSDKGAAAVGMAGSFTDA**-416**	M,R, not H	*This work*
uKHC	Kinesin-1C	NA	Mouse monoclonal	**937-**AVHAVRGGGGGSSNSTHYQK**-956**	M,R,H	*(15) This work*
H2	Kinesin-1A Kinesin-1B Kinesin-1C	Chemicon	Mouse monoclonal	Immunogen: Bovine brain kinesin Epitope within aa **400-600** of Mouse kinesin-1s	M,R,H	*(29)*
L2	KLC1 (Mouse) KLC1/2 (Rat)	Chemicon	Mouse monoclonal	Immunogen: Bovine brain kinesin Epitope: COOH terminus of mouse KLC1	M,R,H?	*(29)*
B2A5	KLC2	NA	Mouse monoclonal	**604-**LSSSSMDLSRRSSLVG**-619**	M,R,H?	*This work*
KLC-AII	KLC1/2	NA	Mouse monoclonal	**307-**KRGKYKEAEP**-316**	M,R,H	*(10)*
63-90	KLC1/2	NA	Mouse monoclonal	Immunogen: Bovine brain kinesin Epitope: Within aa **1-50** of mouse KLC1	M,R,H	*(29, 24,28)*

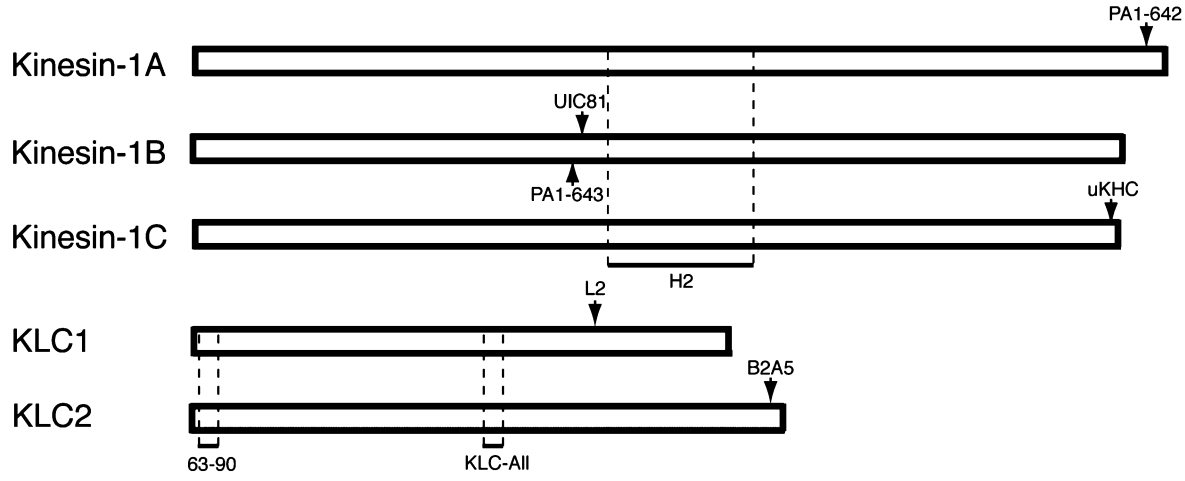

[a] Amino acid numbers for immunizing peptides correspond to murine kinesin-1A (Accession P33175), kinesin-1B (Accession NP_032474), kinesin-1C (Accession P28738), KLC1 (Accession AAC27740), and KLC2 (Accession AAH14845) sequences. A schematic diagram below shows the epitope location of these antibodies (arrowheads) within their respective target proteins. Abbreviations: Sp. Specif., species specificity; Ref., References; NA, not commercially available; ND, not determined; M, mouse; R, rat; H, human. A question mark indicates a species for which the specificity of a given antibody has not been established. Asterisks (*) indicate that polyclonal antibodies generated against the indicated peptide are also available from Abcam.

mammalian protease inhibitor cocktail (Sigma)], as previously described (*32*). Lysates were centrifuged twice for 5 min at 55000 rpm (163640g_{max}) using a TLA 100.3 rotor (Beckman Instruments, Palo Alto, CA). The resulting supernatant fractions were precleared using a mixture of protein G−agarose beads (Pierce) and nonimmune mouse IgG-conjugated Sepharose beads (Jackson Immunoresearch) for 1 h at room temperature. Precleared brain lysate (400 μg) was brought to 1 mL with LB and incubated with 5 μg of the appropriate antibody plus 10 μL of protein G−agarose beads at 4 °C for 3 h. Immunocomplexes were recovered by centrifugation (3000g_{max} for 30 s) and washed four times with 1 mL of LB and once with 50 mM HEPES, pH 7.4. Immunoclomplexes were resuspended in GLB. For immunodepletion experiments in Figure 3B, precleared mouse brain lysates were subjected to three cycles of immunoprecipitation as described above. A 50 μL aliquot of each resultant supernatant was saved for immunoblot analysis after each immunoprecipitation cycle.

Subcellular Fractionation Procedures. A mouse brain was homogenized in 4 mL of HB (0.32 M sucrose, 10 mM HEPES, 5 mM EDTA, pH 7.4). Whole homogenate was centrifuged for 5 min at 1200g_{max}, 5000g_{max}, and 10000g_{max} (10 min each) using a Beckman TLA100.3 rotor. The resulting pellets were discarded, and the final supernatant was centrifuged at 100000g_{max} for 30 min in a Sorval S45A rotor. The membrane pellet obtained [V1 fraction (*23, 31*)] was carefully resuspended in 0.5 mL of HB plus 50% iodixanol using a 27 gauge syringe. Resuspended membranes

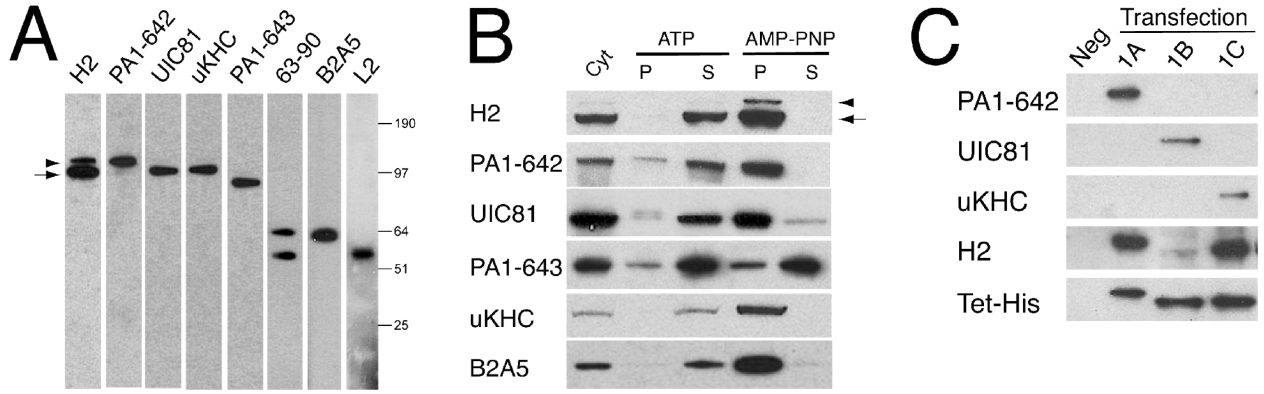

FIGURE 1: Characterization of anti-kinesin-1-specific antibodies. (A) Immunoblot analysis of whole mouse brain lysates using anti-kinesin-1 and anti-KLC antibodies. Anti-kinesin-1A, -1B, and -1C antibodies recognized a single band at the expected molecular mass size (approximately 100–110 kDa). Note the slightly lower mobility of kinesin-1A under these SDS−PAGE conditions. H2 antibody against all kinesin-1s recognizes a band doublet corresponding to kinesin-1A (upper band, arrowhead) and kinesin-1C/B (lower band, arrow). Anti-kinesin-1B PA1–643 antibody recognized a major band with a slower mobility to those recognized by other kinesin-1 antibodies, raising questions against its specificity (see text). (B) Aliquots of mouse brain cytosol (Cyt) were incubated with Taxol and either 2 mM ATP or 2 mM AMP-PNP, a nonhydrolyzable ATP analogue. After 20 min incubation, samples were spun to produce a MT-enriched pellet (P) and a corresponding supernatant (S). In the presence of AMP-PNP, this procedure allows for quantitative recovery of conventional kinesin in association to MT-enriched pellets. Aliquots of each fraction were analyzed by immunoblotting using H2 antibody, and various novel antibodies against kinesin-1s and KLC2 (see Table 1). Note that with the only exception of PA1–643 antibody, all antibodies tested recognized polypeptides which biochemically behave as expected for conventional kinesin. (C) COS-7 cells were transfected with plasmids encoding His-tagged, full-length versions of kinesin-1A, -1B, and -1C and lysed for 24 h after transfection. COS-7 lysates were first normalized to similar kinesin-1 levels using anti-His antibody (Tet-His) and then analyzed by immunoblot using anti-kinesin-1A (PA1–642), anti-kinesin-1B (UIC 81), and anti-kinesin-1C (uKHC) (see Table 1). These antibodies recognized a single band at the expected molecular mass size (approximately 100–110 kDa), and no cross-reactivity with other kinesin-1s was observed. The monoclonal antibody H2 recognized all kinesin-1s, albeit with different affinities (1A > 1C ≫ 1B). After very long exposure of film, a very faint band was recognized by H2 antibody in untransfected (Neg) cells (data not shown). Arrowheads and arrows indicate the positions of kinesin 1A and kinesin-1B/C, respectively.

were placed in a 13 mL centrifuge tube, and a premixed linear gradient from 5% to 23% iodixanol (prepared in HB) was loaded on top. Samples were centrifuged at 150000g_{max} for 3 h using a SW40Ti rotor (Beckman Instruments, Palo Alto, CA). Fifteen fractions were collected from bottom to top using a peristaltic pump. Equal volumes of each fraction were analyzed by SDS−PAGE and immunoblotting. Quantitative immunoblotting was performed as described before (*33*).

RESULTS

Characterization of Anti-Kinesin-1 Antibodies. Both novel and previously described antibodies recognizing specific subunit isotypes of conventional kinesin were rigorously characterized (Table 1). Major differences in the amino and carboxy terminus of KLCs facilitated selection of peptide sequences specific for KLC1 and KLC2. However, the selection of peptide sequences unique to each kinesin-1 was limited by their high degree of sequence homology (*26*). When tested against whole mouse brain lysates, anti-KLC1 (L2) and anti-KLC2 (B2A5) antibodies recognized single bands at 64 and 57 kDa, respectively, whereas the 63–90 antibody recognized both KLC1 and KLC2 (*10, 24*), and these bands comigrated with those recognized by L2 and B2A5, respectively (Figure 1A). Anti-kinesin-1 antibodies recognized immunoreactive bands at the molecular mass expected for kinesin-1s (Figure 1A). The slightly lower mobility of kinesin-1A makes it distinguishable from bands corresponding to kinesin-1B and -1C under these electrophoretic and immunoblotting conditions. H2 antibody recognized a doublet corresponding to kinesin-1A (upper band) and kinesin-1B and -1C combined (lower band) (*18, 29, 34*). Longer exposures with H2 antibody were needed to visualize kinesin-1A, suggesting its levels in whole brain lysates were lower than the combined levels of kinesin-1B and kinesin-1C. Significantly, addressing the identity of kinesin-1s recognized by H2 allowed for the unequivocal identification of kinesin-1A from kinesin-1B/C in fast axonal transport studies previously done by our group (*18*).

The high degree of homology among kinesin-1s prompted us to confirm the specificity of anti-kinesin-1 antibodies taking advantage of a major biochemical characteristic of conventional kinesin: its ability to form a rigor structure with MTs in the presence of AMP-PNP (a nonhydrolyzable analogue of ATP) but not ATP (*35*). Mouse brain cytosolic fractions were incubated with Taxol and either 2 mM ATP or 2 mM AMP-PNP. After 20 min incubation, samples were spun to produce a MT-enriched pellet and a corresponding supernatant (Figure 1B) (*36*). Aliquots of each fraction obtained were analyzed by immunoblotting. Immunoreactive bands recognized by H2, PA1−642, UIC 81, uKHC, L2, B2A5, and KLC-All antibodies were all enhanced in MT-enriched pellets prepared in the presence of AMP-PNP, compared to those prepared in the presence of ATP. Since these properties are identical to those previously reported for conventional kinesin, we concluded that these antibodies effectively recognized their specific target and not other proteins with a similar molecular mass. The only exception was PA1–643, a commercially available antibody against kinesin-1B. PA1–643 recognized a major band with a molecular mass similar to that of kinesin-1B, but this band was present at similar levels in both ATP and AMP-PNP MT-enriched pellets. After long exposures, a very faint band was visualized which behaved as expected for kinesin-1B (data not shown), but this band was undetectable in total

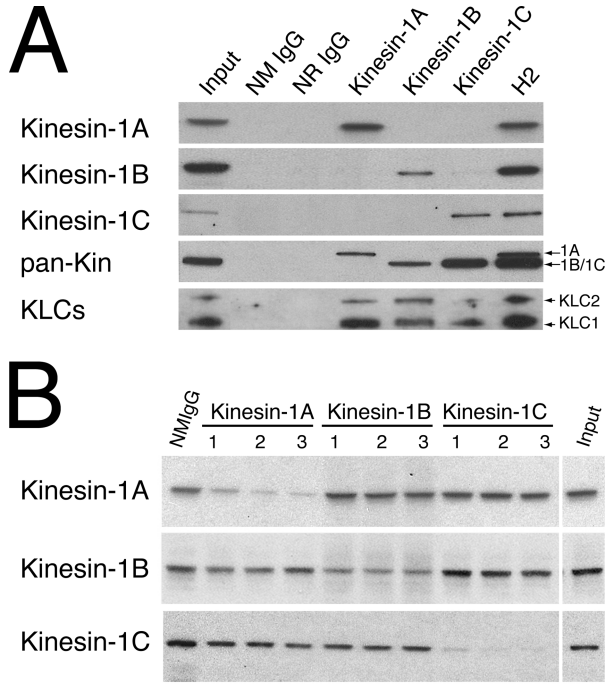

FIGURE 2: Kinesin-1s exist as homodimers in brain tissue. (A) Validated anti-kinesin-1 antibodies were used for immunoprecipitation from mouse brain lysates. Non-immune IgGs were used as controls for immunoprecipitation specificity. A lane loaded with mouse brain lysate (Input) is shown. Immunoblot analysis indicates that each antibody exclusively immunoprecipitated their respective antigen. As expected from its specificity, H2 antibody immunoprecipitated all kinesin-1s. The presence of KLC1 and KLC2 in these immunoprecipitates confirmed the native conditions of the methods herein. Key: NR IgG, normal rabbit IgG; NM IgG, normal mouse IgG. (B) Three rounds of immunoprecipitation were carried out as described in (A), and aliquots of the lysate supernatants obtained after each round were analyzed by immunoblot. Depletion of each kinesin-1A and kinesin-1C from brain lysates does not significantly affect the levels of all other kinesin-1 proteins, indicating that kinesin-1s exist primarily as homodimers.

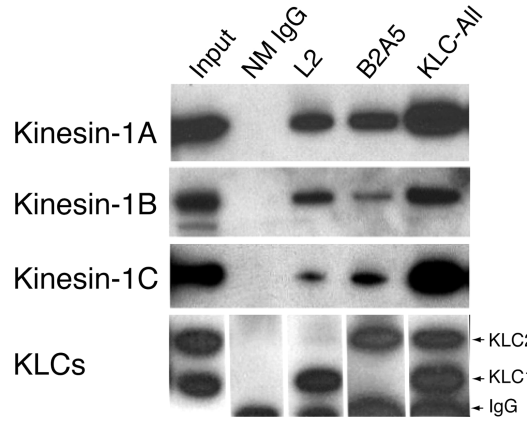

FIGURE 3: Kinesin-1 homodimers interact with both KLC1 and KLC2 homodimers. Immunoblots with 63–90 antibody show that anti-KLC1 (L2) and anti-KLC2 (B2A5) antibodies selectively immunoprecipitated their corresponding antigen, whereas KLC-All antibody raised against the TR domain common to all KLCs immunoprecipitated both. These data confirmed previous reports of KLC homodimerization. Significantly, kinesin-1A, -1B, and -1C could all be found in both anti-KLC1 and anti-KLC2 immunoprecipitates, suggesting there is no specificity in the interactions between KLCs and kinesin-1 homodimers.

brain lysates. As a result of this cross-reactivity, the PA1–643 antibody is not well suited for analysis of kinesin-1B in cell or tissue samples. This observation highlights the importance of proper antibody validation in studies involving highly homologous polypeptides. We next examined potential cross-reactivities among kinesin-1 antibodies. The production of bacterially expressed full-length recombinant kinesin-1 polypeptides in bacteria mainly resulted in the formation of truncated species of lower molecular mass (*37*), thus complicating the identification of properly folded, full-length kinesin-1 polypeptides that would enable appropriate antibody characterization. To circumvent these issues, anti-kinesin-1 antibodies were reacted with lysates derived from COS-7 cells transfected with cDNAs coding for 6-His-tagged, full-length mouse kinesin-1A, kinesin-1B, or kinesin-1C (Figure 1C). COS-7 cell lysates were normalized to similar levels of overexpressed kinesin-1s using an antibody against their 6-His tag. Whereas endogenous kinesin-1 levels were close to the levels of detection (*38*), exogenously expressed kinesin-1s migrated as single full-length polypeptide bands of approximately 100–110 kDa (Figure 1C). From this approach, antibodies specific for each kinesin-1 were identified (PA1−642, UIC 81, and uKHC for kinesin-1A, -1B, and -1C, respectively). In agreement with previous reports (*26*), the widely used monoclonal H2 antibody was found to recognize all kinesin-1s, albeit with different affinities (1A > 1C ≫ 1B; data not shown).

Conventional Kinesin Is Composed of Kinesin-1 Homodimers. Determining all potential combinations among conventional kinesin subunits has been limited by the lack of well-characterized antibodies that selectively recognize specific subunits. Anti-kinesin-1 antibodies described above were used to immunoprecipitate conventional kinesin from mouse brain under native conditions (*26*) (*32*) (Figure 2). As expected, each anti-kinesin-1 antibody immunoprecipitated its corresponding kinesin-1 target protein (Figure 2A). The only exception was the H2 antibody, which immunoprecipitated all kinesin-1s, albeit with different affinities (data not shown). Significantly, we found no evidence of kinesin-1 heterodimers, as only one kinesin-1 type could be detected in these immunoprecipitates with kinesin-1-specific antibodies. Analysis of these immunoprecipitates using the 63–90 antibody [recognizing both KLC1 and KLC2 (24, 39)] confirmed the native conditions of our immunoprecipitation methods. We did not observe a preferred association between KLC1 or KLC2 with a specific set of kinesin-1s (see below).

To enhance our ability to detect potentially low levels of kinesin-1 heterodimers, we performed three rounds of immunoprecipitation (as described above) and evaluated the levels of other kinesin-1s remaining in immunodepleted lysates (Figure 2B). If kinesin-1s associated with each other to form heterodimers, a prediction could be made that depletion of a given kinesin-1 would have an impact on the total levels of other kinesin-1s remaining in the lysate (*32*). Although both kinesin-1A and kinesin-1C were significantly depleted from lysates after three rounds of immunoprecipitation, their depletion did not affect the levels of other kinesin-1s in the remaining supernatants. Anti-kinesin-1B antibodies only immunoprecipitated a small fraction of total kinesin-1B present in mouse brain lysates (Figure 2A), but this amount was not increased after three rounds of immunoprecipitation, suggesting the UIC 81 epitopes might be cryptic in a significant fraction of kinesin-1B. Regardless, depletion of a specific kinesin-1 from brain lysates did not

affect the levels of other kinesin-1s in supernatant fractions, suggesting that conventional kinesin from brain is exclusively composed of kinesin-1 homodimers.

Kinesin-1 Homodimers Show No Specificity in Their Interaction with KLC Homodimers. To characterize interactions among kinesin-1 and KLCs further, antibodies specific for each KLC were used to immunoprecipitate conventional kinesin holoenzymes (Figure 3). Whereas KLC-All antibody immunoprecipiated both KLC1 and KLC2 (*10*), KLC1 and KLC2 were selectively immunoprecipitated using monoclonal antibodies L2 and B2A5, respectively (see Table 1). Immunoblotting analysis of these immunoprecipitates using the 63–90 antibody (which recognizes both KLC1 and KLC2) found no evidence of KLC heterodimers, consistent with previous reports (*24, 27*). Interestingly, all kinesin-1s were detected in both KLC1 and KLC2 immunoprecipitates, indicating that there is no selectivity in the interaction of KLC homodimers and kinesin-1 homodimers. The detection of all kinesin-1s in each KLC immunoprecipitate indicated that the detection of single kinesin-1s in the anti-kinesin-1 immunoprecipitates above (Figure 2A) was not due to potential dissociation of kinesin-1 heterodimers during immunoprecipitation. These data, along with the recovery of both KLC1 and KLC2 in all kinesin-1 immunoprecipitates (Figure 2A), indicated that kinesin-1 homodimers can associate with either KLC1 or KLC2 homodimers and suggested the existence of six different forms of conventional kinesin in brain, as defined by their subunit composition.

Biochemically Heterogeneous Forms of Conventional Kinesin Associate to Different MBOs. Biochemical fractionation approaches provided a useful method to gain insights on MBO cargoes transported by various members of the kinesin superfamily (*30, 40*). Our findings above led us to examine potential correlations in the distribution of specific subunits of conventional kinesin and various MBO cargoes. To this end, a biochemically heterogeneous microsomal membrane fraction was first obtained from mouse brain by subcellular fractionation, under conditions that help preserve kinesin-1 association with membranes (*31, 41*). Microsomal membranes were further fractionated by iodixanol density gradient centrifugation methods, and several fractions along the iodixanol gradient were analyzed by immunoblotting using antibodies against kinesin-1s, KLCs, and various membrane-associated proteins corresponding to different MBO markers (Figure 4). Consistent with differences in their buoyancy, membrane fractions obtained along the gradient showed significant differences in their biochemical composition (Figure 4A). Such differential distribution of organelle markers was consistent with other reports using gradient fractionation procedures (*30, 40*). Quantitation of immunoblots revealed that despite the significant overlap in their distribution, kinesin-1A, -1B, and -1C showed distinct distribution profiles along the iodixanol gradient (Figure 4B). Most kinesin-1B was recovered in a sharp peak corresponding to the highest iodixanol concentration in the gradient (22–23%), partially overlapping with the distribution of the synaptic protein marker synapsin I. The distributions of kinesin-1A and kinesin-1C followed a bimodal pattern, peaking at both 12% (peak 1) and 19% (peak 2) iodixanol concentrations. However, the relative enrichments of kinesin-1A and kinesin-1C in peak 1 and peak 2 were clearly different. Specifically, levels of kinesin-1A in peaks 1 and

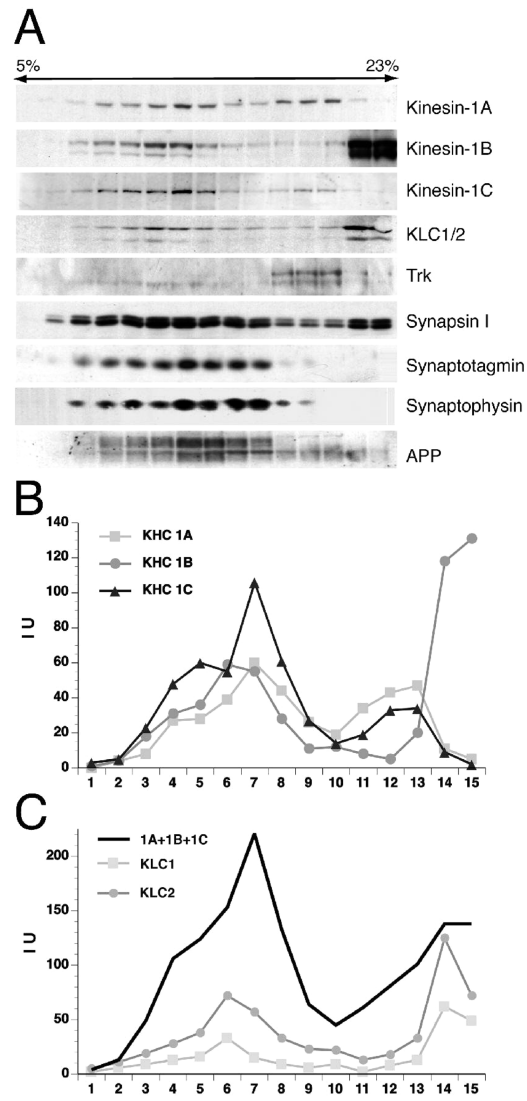

FIGURE 4: Biochemically heterogeneous forms of conventional kinesin associate to different MBOs. (A) Microsomal membranes from mouse brain were fractionated by iodixanol density gradient centrifugation, and several fractions along the iodixanol gradient were analyzed by immunoblotting using antibodies against kinesin-1s, KLCs, and various membrane-associated proteins corresponding to different MBO markers. (B, C) Quantitation of blots in (A) shows different distribution profiles of kinesin-1s (B) but not KLCs (C) along the iodixanol gradient, suggesting a role of kinesin-1s in the targeting of conventional kinesin holoenzymes to biochemically heterogeneous membrane-bounded organelle cargoes. The distribution of all kinesin-1s plotted together (1A + 1B + 1C) resembled that of KLCs, confirming the heterotetrameric composition of conventional kinesin in association to these MBOs. IU = intensity units.

2 were comparable, whereas most kinesin-1C was present in peak 1. Interestingly, peak 1 comprised a significant fraction of the synaptic vesicle (SV) proteins synaptophysin and synaptotagmin, as well as that of glycosylated, neuron-specific forms of amyloid precursor protein (APP), whereas peak 2 displayed a striking codistribution with neurotrophin (trk) receptors. Remarkably, no clear segregation of KLC1 and KLC2 along the gradient was observed under these experimental conditions (Figure 4C), although their distribution closely matched the overall profile of all kinesin-1s together (total kinesin-1s). Taken collectively, these data suggest that biochemically heterogeneous forms of conventional kinesin associate with different MBO types, in a

manner that correlates with their kinesin-1 composition. However, the complexity of these profiles suggests that many neuronal proteins may be transported in several classes of MBOs, with the bulk in one class and smaller amounts in other classes of MBOs.

DISCUSSION

Since the original discovery of conventional kinesin (*35*), it has become increasingly clear that this motor is involved in the transport of various MBOs along axons. MBOs found in association with conventional kinesin include synaptic vesicles, lysosomes, mitochondria, coated vesicles, and post-Golgi carriers (*19, 21*). Even though conventional kinesin interacts with such heterogeneous MBO types, it does not associate with all types of cellular membranes. For example, conventional kinesin copurifies with mitochondria and synaptic vesicles but was almost undetectable in some other membrane fractions (i.e., nuclei), suggesting that the targeting of conventional kinesin to the MBOs above is specific and selective (*21*). Further strengthening this argument, immunoelectron microscopic studies showed a discrete localization of conventional kinesin on MBO surfaces (*21*). These observations suggest the existence of cellular mechanisms, which allow for the selective targeting of conventional kinesin to structurally and biochemically heterogeneous MBO cargoes.

Biochemical diversity in kinesin-1 and KLC subunits was first recognized as methods for the purification of brain kinesin were being developed (*34*). More recently, cloning (*8, 42*) and genomic information confirmed and extended these findings, identifying the whole complement of kinesin-1 and KLC genes in mammals. Thorough analysis of the mouse genome confirmed the existence of three kinesin-1 and three KLC gene products (*1*). From these, all kinesin-1s and two KLCs [KLC1, KLC2 (*24*)] are expressed in nervous tissue (*2*). Although the precise significance of this heterogeneity in conventional kinesin subunits from brain is unknown, it likely reflects functional differences (*13*). Supporting this idea, kinesin-1s showed significant differences in their tissue distribution (*25, 26*), developmental expression profiles (*43*), and transport rates (*18*), and specific KLC isoform variants are found in association to different MBOs (*11, 12, 44*). From these observations, it became apparent that determining the precise composition of conventional kinesin from brain represented a critical step toward an understanding of mechanisms underlying the targeting of conventional kinesin to different MBOs.

As a first step, antibodies specific for each conventional kinesin subunit were generated and/or characterized, and their specificities were validated using various independent approaches. When tested against mouse brain lysates, these antibodies reacted with polypeptides migrating at the molecular mass expected for each subunit. However, such criteria alone proved insufficient, given the high degree of homology among kinesin-1 polypeptides. Antibodies were validated, taking advantage of the well-established biochemical property of conventional kinesin to form a rigor structure with MTs in the presence of the nonhydrolyzable ATP analogue AMP-PNP (*35*). Immunoreactive bands recognized by these antibodies were significantly enriched in MT pellets prepared in the presence of AMP-PNP, but not ATP, thus validating PA1–642, UIC 81, uKHC, L2, and B2A5 antibodies. Importantly, not all antibodies tested met the criteria above. For example, a commercially available polyclonal antibody against kinesin-1B (PA1–643) recognized a prominent band at approximately 100 kDa in mouse brain lysates, but this band partitioned similarly to MT-enriched pellets in a manner independent of the nucleotide present. Finally, potential cross-reactivity among anti-kinesin-1 antibodies was evaluated by immunoblotting using lysates derived from COS-7 cells transfected with full-length cDNA constructs coding for kinesin-1A, -1B, and -1C. COS-7 cells were chosen because, unlike bacteria, these cells efficiently express transfected full-length kinesin-1s (*38*). Also, these cells express low levels of endogenous kinesin-1. Supporting this idea, long exposures were needed with the high-affinity H2 antibody to detect kinesin-1 in untransfected COS cells (data not shown). This strategy allowed us to confirm the selectivity of anti-kinesin-1 antibodies against their specific kinesin-1 target.

Having identified antibodies that selectively recognize a conventional kinesin subunit, we evaluated all possible subunit combinations present in endogenous conventional kinesin from brain using immunoprecipitation approaches (*32*) (*45*). As expected, each anti-kinesin-1 antibody immunoprecipitated their appropriate target kinesin-1, albeit with different affinities. Coimmunoprecipitation of KLCs with the kinesin-1 antibodies confirmed the native, nondenaturing conditions of our immunoprecipitation procedure (*32*). Significantly, no kinesin-1 other than the one specific for each antibody could be detected, indicating that conventional kinesin holoenzymes precipitated by these antibodies are composed of kinesin-1 homodimers. Immunodepletion experiments further tested this possibility. If a significant fraction of endogenous kinesin-1s can associate to form heterodimers *in vivo*, a prediction could be made that depletion of a specific kinesin-1 form from brain lysates would impact on the levels of other kinesin-1s remaining in these lysates. Significantly, nearly complete depletion of kinesin-1A and kinesin-1C from mouse lysates did not affect the total levels of other kinesin-1s. Although kinesin-1B could not be completely immunodepleted, its levels were unaffected by the depletion of kinesin-1A and kinesin-1C. Taken together, these results indicated that endogenous conventional kinesin from brain is composed exclusively of kinesin-1 homodimers.

Our findings on kinesin-1 homodimerization here sharply contrast with a previous report showing that different kinesin-1s can associate to form heterodimers (*26*). This notion, however, was inconsistent with the large differences in tissue distribution, relative levels, and cellular functions proposed for each kinesin-1 (*26*), as well as differences in their transport rates (*18*), the phenotypic manifestation of each kinesin-1 knockout (*26, 46, 47*), and the preferred association of selected kinesin-1s to various protein effectors (*25*), all observations which strongly suggested unique roles for each kinesin-1 in the nervous system. Differences in antibody specificities could explain these disparate results.

Previous reports indicated that KLCs interact with each other to form homodimers of the same KLC type (*24*) and isoform (*27*). These findings were confirmed and further extended by the studies here. Specifically, we found that all three kinesin-1s were coimunoprecipitated with each KLC,

indicating that KLC1 and KLC2 homodimers can interact with all three possible kinesin-1 homodimers. These data confirmed previous reports of KLC homodimerization (*24*) and were consistent with the high degree of homology found in the KLC-binding domain among kinesin-1s. Throughout our studies, some small variability was observed in the amounts of each kinesin-1 coimmunoprecipitated with KLC1 and KLC2 (data not shown). Potential sources of variability include the relative abundance of different kinesin-1s in different areas of the brain (data not shown). Because immunoprecipitations were done using whole brain lysates, small variations in homogenization could contribute to the variability above. Our results allowed us to conclude unequivocally that each kinesin-1 has the ability to bind to either KLC1 or KLC2 but do not permit definitive statements on the relative affinities of each KLC for each kinesin-1. This later issue clearly requires different experimental approaches, currently ongoing in our laboratory. Taken together, data obtained from kinesin-1 and KLC immunoprecipitation experiments suggest the existence of six variants of conventional kinesin, as defined by their subunit compositions (kinesin-1A/KLC1, kinesin-1A/KLC2, kinesin-1B/KLC1, kinesin-1B/KLC2, kinesin-1C/KLC1, and kinesin-1C/KLC2). However, KLC1 transcripts have been shown to undergo alternative splicing that results in the generation of numerous KLC1 isoforms (*8, 11*), so the actual combination of kinesin subunits that may produce functionally diverse holoenzymes exceeds the number estimated from the gene product composition alone and may expand the repertoire of functions possible for a given kinesin-1.

We next examined preferred associations between biochemically heterogeneous MBOs and specific conventional kinesin subunits using subcellular fractionation approaches. Significantly, kinesin-1A, -1B, and -1C showed different distribution profiles along continuous iodixanol gradients, which were consistent with association of specific kinesin-1s to biochemically heterogeneous MBOs. In contrast to kinesin-1s, KLC1 and KLC2 displayed nearly identical distribution profiles under these experimental conditions. Consistent with the results above, kinesin-1s, but not KLCs, displayed major differences in their transport kinetics *in vivo*, and these differences correlated with association to different MBOs (*18*). Taken together, these data suggested that kinesin-1s play a role in the targeting of conventional kinesin variants to different MBOs. Such a claim is consistent with ultrastructural observations showing extensive association of conventional kinesin's heavy chains with their membranous cargoes (*16*). Although differences in the subcellular distribution of KLC1 and KLC2 were not obvious in subcellular fractionation experiments here, immunolocalization experiments in cultured cells showed different MBO localizations for each KLC1 isoform (refs *11* and *12*; Stenoien and Brady, unpublished observations), suggesting a role for the variable COOH terminus of KLCs in the targeting of conventional kinesin to selected MBOs (*13*). Although a role of the KLC's TR domain in the tight binding of conventional kinesin to membranes is well established (*10*), it is unlikely that this domain plays a role in the targeting of conventional kinesin, given its invariable presence in all KLCs (*9, 10*). The TR domain likely contributes to the tight binding of conventional kinesins to MBOs. The available experimental evidence suggests that both the variable globular tail domain of kinesin-1s and the extreme carboxy termini of KLCs play a role in the selective targeting of conventional kinesin variants to selected MBOs (*9, 13*). Further work is needed to establish the precise functional role of each subunit in this process.

The localized delivery of selected MBOs at specific neuronal and axonal subdomains underlies the ability of neurons to receive and transmit chemical information. Significantly, our data provide a conceptual basis for the transport regulation of specific MBO populations conveyed by conventional kinesin in neurons (*23*). Indeed, various reports indicate the existence of both kinesin-1 and KLC-specific regulatory mechanisms, which are consistent with our findings of kinesin-1 and KLC homodimerization properties described here. For example, various proteins have been reported which selectively associate to specific kinesin-1s (*15, 25*). Also, various protein kinases have been identified, which selectively regulate kinesin-1 (*33*) or KLC-related activities (*48*), and these kinases phosphorylate selected kinesin-1 and KLC polypeptides (Morfini and Brady, unpublished observations). Subunit-specific regulatory mechanisms could allow for the selective, nonpromiscuous regulation of conventional kinesin variants in association to specific MBO cargoes, as well as the delivery of such cargoes to discrete subcellular locations (*23*). Finally, our findings here also have implications for selected aspects of neuronal dysfunction in the context of human diseases, since alterations in regulatory pathways for conventional kinesin-based motility are being increasingly recognized as important pathogenic lesions in various neurodegenerative diseases (*49–51*).

ACKNOWLEDGMENT

The authors thank Dongyan Huang and Oscar Buzzio for excellent technical assistance.

REFERENCES

1. Miki, H., Setou, M., Kaneshiro, K., and Hirokawa, N. (2001) All kinesin superfamily protein, KIF, genes in mouse and human. *Proc. Natl. Acad. Sci. U.S.A. 98*, 7004–7011.
2. Miki, H., Setou, M., and Hirokawa, N. (2003) Kinesin superfamily proteins (KIFs) in the mouse transcriptome. *Genome Res. 13*, 1455–1465.
3. Wagner, M. C., Pfister, K. K., Brady, S. T., and Bloom, G. S. (1991) Purification of kinesin from bovine brain and assay of microtubule-stimulated ATPase activity. *Methods Enzymol. 196*, 157–175.
4. Bloom, G. S., Wagner, M. C., Pfister, K. K., and Brady, S. T. (1988) Native structure and physical properties of bovine brain kinesin and identification of the ATP-binding subunit polypeptide. *Biochemistry 27*, 3409–3416.
5. Hirokawa, N., Pfister, K. K., Yorifuji, H., Wagner, M. C., Brady, S. T., and Bloom, G. S. (1989) Submolecular domains of bovine brain kinesin identified by electron microscopy and monoclonal antibody decoration. *Cell 56*, 867–878.
6. Kuznetsov, S. A., Vaisberg, E. A., Shanina, N. A., Magretova, N. A., Chernyak, N. M., and Gelfand, V. I. (1988) The quatenary structure of bovine brain kinesin. *EMBO J. 7*, 353–356.
7. Lawrence, C. J., Dawe, R. K., Christie, K. R., Cleveland, D. W., Dawson, S. C., Endow, S. A., Goldstein, L. S., Goodson, H. V., Hirokawa, N., Howard, J., Malmberg, R. L., McIntosh, J. R., Miki, H., Mitchison, T. J., Okada, Y., Reddy, A. S., Saxton, W. M., Schliwa, M., Scholey, J. M., Vale, R. D., Walczak, C. E., and Wordeman, L. (2004) A standardized kinesin nomenclature. *J. Cell Biol. 167*, 19–22.
8. Cyr, J. L., Pfister, K. K., Bloom, G. S., Slaughter, C. A., and Brady, S. T. (1991) Molecular genetics of kinesin light chains: Generation of isoforms by alternative splicing. *Proc. Natl. Acad. Sci. U.S.A. 88*, 10114–10118.

9. Wozniak, M. J., and Allan, V. J. (2006) Cargo selection by specific kinesin light chain 1 isoforms. *EMBO J. 25*, 5457–5468.
10. Stenoien, D. S., and Brady, S. T. (1997) Immunochemical analysis of kinesin light chain function. *Mol. Biol. Cell 8*, 675–689.
11. Khodjakov, A., Lizunova, E. M., Minin, A. A., Koonce, M. P., and Gyoeva, F. K. (1998) A specific light chain of kinesin associates with mitochondria in cultured cells. *Mol. Biol. Cell 9*, 333–343.
12. Gyoeva, F. K., Bybikova, E. M., and Minin, A. A. (2000) An isoform of kinesin light chain specific for the Golgi complex. *J. Cell. Sci. 113* (Part 11), 2047–2054.
13. Brady, S. T. (1995) A kinesin medley: Biochemical and functional heterogeneity. *Trends Cell Biol. 5*, 159–164.
14. Diefenbach, R. J., Mackay, J. P., Armati, P. J., and Cunningham, A. L. (1998) The C-terminal region of the stalk domain of ubiquitous human kinesin heavy chain contains the binding site for kinesin light chain. *Biochemistry 37*, 16663–16670.
15. Huang, J. D., Brady, S. T., Richards, B. W., Stenoien, D., Resau, J. H., Copeland, N. G., and Jenkins, N. A. (1999) Direct interaction of two different transport motors and implications for vesicle transport. *Nature 397*, 267–270.
16. Hirokawa, N., Bloom, G. S., and Vallee, R. B. (1985) Cytoskeletal architecture and immunocytochemical localization of microtubule-associated proteins in regions of axons associated with rapid axonal transport: the beta,beta′-iminodipropionitrile-intoxicated axon as a model system. *J. Cell Biol. 101*, 227–239.
17. Morfini, G., Stenoien, D. L., and Brady, S. T. (2005) *Basic Neurochemistry*, 7th ed., Publisher, Address.
18. Elluru, R., Bloom, G. S., and Brady, S. T. (1995) Fast axonal transport of kinesin in the rat visual system: functionality of the kinesin heavy chain isoforms. *Mol. Biol. Cell 6*, 21–40.
19. Jaulin, F., Xue, X., Rodriguez-Boulan, E., and Kreitzer, G. (2007) Polarization-dependent selective transport to the apical membrane by KIF5B in MDCK cells. *Dev. Cell 13*, 511–522.
20. Feiguin, F., Ferreira, A., Kosik, K. S., and Caceres, A. (1994) Kinesin-mediated organelle translocation revealed by specific cellular manipulations. *J. Cell Biol. 127*, 1021–1039.
21. Leopold, P. L., McDowall, A. W., Pfister, K. K., Bloom, G. S., and Brady, S. T. (1992) Association of kinesin with characterized membrane-bounded organelles. *Cell Motil. Cytoskeleton 23*, 19–33.
22. Boiko, T., Rasband, M. N., Levinson, S. R., Caldwell, J. H., Mandel, G., Trimmer, J. S., and Matthews, G. (2001) Compact myelin dictates the differential targeting of two sodium channel isoforms in the same axon. *Neuron 30*, 91–104.
23. Morfini, G., Szebenyi, G., Richards, B., and Brady, S. T. (2001) Regulation of kinesin: implications for neuronal development. *Dev. Neurosci. 23*, 364–376.
24. Rahman, A., Friedman, D. S., and Goldstein, L. S. (1998) Two kinesin light chain genes in mice. *J. Biol. Chem. 273*, 15395–15403.
25. Cai, Y., Singh, B. B., Aslanukov, A., Zhao, H., and Ferreira, P. A. (2001) The docking of kinesins, KIF5B and KIF5C, to Ran-binding protein 2 (RanBP2) is mediated via a novel RanBP2 domain. *J. Biol. Chem. 276*, 41594–41602.
26. Kanai, Y., Okada, Y., Tanaka, Y., Harada, A., Terada, S., and Hirokawa, N. (2000) KIF5C, a novel neuronal kinesin enriched in motor neurons. *J. Neurosci. 20*, 6374–6384.
27. Gyoeva, F. K., Sarkisov, D. V., Khodjakov, A. L., and Minin, A. A. (2004) The tetrameric molecule of conventional kinesin contains identical light chains. *Biochemistry 43*, 13525–13531.
28. Pigino, G., Morfini, G., Mattson, M. P., Brady, S. T., and Busciglio, J. (2003) Alzheimer's presenilin 1 mutations impair kinesin-based axonal transport. *J. Neurosci. 23*, 4499–4508.
29. Pfister, K. K., Wagner, M. C., Stenoien, D., Bloom, G. S., and Brady, S. T. (1989) Monoclonal antibodies to kinesin heavy and light chains stain vesicle-like structures, but not microtubules, in cultured cells. *J. Cell Biol. 108*, 1453–1463.
30. Morfini, G., Quiroga, S., Rosa, A., Kosik, K., and Caceres, A. (1997) Suppression of KIF2 in PC12 cells alters the distribution of a growth cone nonsynaptic membrane receptor and inhibits neurite extension. *J. Cell Biol. 138*, 657–669.
31. Morfini, G., Tsai, M., Szebenyi, G., and Brady, S. T. (2000) Approaches to study interactions between kinesin motors and membranes, in *Kinesin Protocols* (Vernos, I., Ed.) pp 147–162, Humana Press, Totowa, NJ.
32. Lazarov, O., Morfini, G. A., Lee, E. B., Farah, M. H., Szodorai, A., Koliatsos, V., Kins, S., Lee, V. M.-Y., Wong, P. C. Y., Price, D. L., Brady, S. T., and Sisodia, S. S. (2005) Axonal transport, amyloid precursor protein, kinesin-1, and the processing apparatus: revisited. *J. Neurosci. 25*, 2386–2395.
33. Morfini, G., Pigino, G., Szebenyi, G., You, Y., Pollema, S., and Brady, S. T. (2006) JNK mediates pathogenic effects of polyglutamine-expanded androgen receptor on fast axonal transport. *Nat. Neurosci. 9*, 907–916.
34. Wagner, M. C., Pfister, K. K., Bloom, G. S., and Brady, S. T. (1989) Copurification of kinesin polypeptides with microtubule-stimulated Mg-ATPase activity and kinetic analysis of enzymatic processes. *Cell Motil. Cytoskeleton 12*, 195–215.
35. Brady, S. T. (1985) A novel brain ATPase with properties expected for the fast axonal transport motor. *Nature 317*, 73–75.
36. Lasek, R. J., and Brady, S. T. (1984) Adenylyl imidodiphosphate (AMPPNP), a nonhydrolyzable analogue of ATP, produces a stable intermediate in the motility cycle of fast axonal transport. *Biol. Bull. 167*, 503.
37. Cho, K. I., Cai, Y., Yi, H., Yeh, A., Aslanukov, A., and Ferreira, P. A. (2007) Association of the kinesin-binding domain of RanBP2 to KIF5B and KIF5C determines mitochondria localization and function. *Traffic 8*, 1722–1735.
38. Verhey, K. J., Lizotte, D. L., Abramson, T., Barenboim, L., Schnapp, B. J., and Rapoport, T. A. (1998) Light chain-dependent regulation of kinesin's interaction with microtubules. *J. Cell Biol. 143*, 1053–1066.
39. Pigino, G., Pelsman, A., Mori, H., and Busciglio, J. (2001) Presenilin-1 mutations reduce cytoskeletal association, deregulate neurite growth, and potentiate neuronal dystrophy and tau phosphorylation. *J. Neurosci. 21*, 834–842.
40. Okada, Y., Yamazaki, H., Sekine-Aizawa, Y., and Hirokawa, N. (1995) The neuron-specific kinesin superfamily protein KIF1A is a unique monomeric motor for anterograde axonal transport of synaptic vesicle precursors. *Cell 81*, 769–780.
41. Tsai, M.-Y., Morfini, G., Szebenyi, G., and Brady, S. T. (2000) Modulation of kinesin-vesicle interactions by Hsc70: Implications for regulation of fast axonal transport. *Mol. Biol. Cell 11*, 2161–2173.
42. Aizawa, H., Sekine, Y., Takemura, R., Zhang, Z., Nangaku, M., and Hirokawa, N. (1992) Kinesin superfamily in murine central nervous system. *J. Cell Biol. 119*, 1287–1296.
43. Vignali, G., Lizier, C., Sprocati, M. T., Sirtori, C., Battaglia, G., and Navone, F. (1997) Expression of neuronal kinesin heavy chain is developmentally regulated in the central nervous system of the rat. *J. Neurochem. 69*, 1840–1849.
44. Brady, S. T., and Pfister, K. K. (1991) in *Motor Proteins* (Kendrick-Jones, J., and Cross, R. A., Eds.) pp 103–108, The Company of Biologists, Ltd., Cambridge, England.
45. Morfini, G., Pigino, G., and Brady, S. T. (2007) Approaches to kinesin-1 phosphorylation. *Methods Mol. Biol. 392*, 51–69.
46. Xia, C. H., Roberts, E. A., Her, L. S., Liu, X., Williams, D. S., Cleveland, D. W., and Goldstein, L. S. (2003) Abnormal neurofilament transport caused by targeted disruption of neuronal kinesin heavy chain KIF5A. *J. Cell Biol. 161*, 55–66.
47. Tanaka, Y., Kanai, Y., Okada, Y., Nonaka, S., Takeda, S., Harada, A., and Hirokawa, N. (1998) Targeted disruption of mouse conventional kinesin heavy chain, kif5B, results in abnormal perinuclear clustering of mitochondria. *Cell 93*, 1147–1158.
48. Morfini, G., Szebenyi, G., Elluru, R., Ratner, N., and Brady, S. T. (2002) Glycogen synthase kinase 3 phosphorylates kinesin light chains and negatively regulates kinesin-based motility. *EMBO J. 23*, 281–293.
49. Morfini, G., Pigino, G., Beffert, U., Busciglio, J., and Brady, S. T. (2002) Fast axonal transport misregulation and Alzheimer's disease. *Neuromol. Med. 2*, 89–99.
50. Morfini, G., Pigino, G., and Brady, S. T. (2005) Polyglutamine expansion diseases: Failing to deliver. *Trends Mol. Med. 11*, 64–70.
51. Morfini, G., Pigino, G., Opalach, K., Serulle, Y., Moreira, J. E., Sugimori, M., Llinas, R. R., and Brady, S. T. (2007) 1-Methyl-4-phenylpyridinium affects fast axonal transport by activation of caspase and protein kinase C. *Proc. Natl. Acad. Sci. U.S.A. 104*, 2442–2447.

BI702445J